Boundary-Forced Nonlinear Planetary Radiation

PAOLA MALANOTTE-RIZZOLI

Department of Earth, Atmospheric and Planetary Sciences, Massachusetts Institute of Technology, Cambridge, MA 02139

(Manuscript received 21 October 1983, in final form 13 March 1984)

ABSTRACT

In recent years there has been renewed interest in the Gulf Stream system and its interaction with the mesoscale oceanic eddy field. An important question, not yet adequately addressed, concerns the possible generation mechanisms of the mesoscale eddy field and, in general, the problem of radiation of mesoscale energy from a meandering current. This problem has been investigated in a variety of studies, the basic result of which is that, in the quiescent ocean, the far field can transmit energy radiated by a meandering northern current only if the latter has a westward phase speed. All the proposed models are, however, linear. Nonlinear effects may be expected to modify the above results, as indicated by numerical experiments carried out with fully nonlinear models.

In the present study, the question is addressed in the context of a fully nonlinear but simple model, the quasi-geostrophic equivalent barotropic potential vorticity equation in a zonal channel over variable relief. The meandering current is idealized as a moving northern boundary. First, the case of free nonlinear Rossby wave radiation is studied. Solutions are found in both the weak and high-amplitude limit. The latter solutions are symmetric monopoles with closed recirculation regions, strongly similar to the ring shapes observed to be shed by the Gulf Stream.

In the boundary-forced case, the weakly nonlinear problem is thoroughly analyzed and boundary-forced, equilibrium nonlinear solutions are found. The basic effects of nonlinearity can be summarized as follows:

1) Nonlinearity allows for the production of nonlinear radiation in the interior field through a resonance mechanism. The resonant, equilibrium-forced solutions obey a forced Korteweg–de Vries (KdV) equation and admit, for a specific choice of the forcing, two equilibrium amplitudes.

2) Allowing for a slow time modulation of the northern boundary wave, the resonant interior response obeys the time-dependent KdV equation. Numerical experiments show that an initial condition corresponding to the steady equilibrium solution previously found evolves with soliton production in the region affected by the forcing. Thus, the interior response undergoes, on a long time scale, a nonlinear deterministic cascade process leading to nonlinear radiation of shorter wavelength.

3) In the limit of high nonlinearity, and for long-wave radiation, it can be shown analytically that the cross-channel structure of the interior field is very different from the structure allowed by the corresponding linear model. In the linear case, over an essentially northward-sloping relief, an eastward-moving boundary excites a response which, at best, has an oscillatory nature only in some interior, limited region, while exponentially decaying near the northern boundary. Conversely, in the highly nonlinear case the resonant response is oscillatory, i.e., radiating near the northern boundary. For sufficiently high nonlinearity, the excited eddy will have closed recirculation regions which may detach and propagate away from the boundary like Gulf Stream rings.

1. Introduction

In recent years there has been renewed interest in the Gulf Stream system and its interaction with the mesoscale oceanic eddy field. From the experimental evidence accumulated in experiments like MODE and POLYMODE, important questions emerge which have not yet been adequately treated even in the context of simple theoretical models. One of these questions concerns the possible generation mechanism of the mesoscale eddy field and, in the limit of high-amplitude radiation, the formation of ring-like structures from an eastward-meandering jet, like those observed to emerge from the Gulf Stream.

This question is related to the general problem of the radiation of mesoscale energy from a meandering current, which has been studied by several authors. Flierl *et al.* (1975) examined the behavior of semi-infinite domains driven by boundary forcing, using the linear barotropic vorticity equation on the β-plane. Pedlosky (1977) treated the same problem with a two-layer quasi-geostrophic model including a mean current. Harrison and Robinson (1979) studied the question of radiation from a northern boundary into a finite domain, with zero boundary conditions at the meridional boundaries which make it rather different from the infinite northern wall problem. In the latter case, the basic result is that in the quiescent ocean the far field can transmit energy radiated by the northern boundary only if it has a westward phase speed.

All these models are, however, linear. Nonlinear effects may be expected to modify the above results,

as indicated by numerical experiments carried out with fully nonlinear models in which mesoscale radiation is observed to be excited and to radiate away from an eastward-moving jet (Holland, 1978; Ikeda, 1981; Ikeda and Apel, 1981).

The above problem is investigated here in the context of a fully nonlinear, although simple, model in which the meandering current again is idealized as a moving northern boundary. In Section 2 we assess the model, namely the quasi-geostrophic equivalent barotropic potential vorticity equation in a zonal channel over variable topography, and find free nonlinear wave solutions in different parameter ranges.

In Section 3 the problem of boundary-forced nonlinear radiation is thoroughly examined in the weakly nonlinear parameter range. Nonlinearity allows for the production of radiation in the interior field through a resonance mechanism. The resonant equilibrium-forced solutions obey a forced Korteweg–de Vries (KdV) equation and admit, for a specific choice of the forcing, two equilibrium amplitudes.

Two further effects of nonlinearity can be demonstrated analytically. First, in the limit of high nonlinearity, and for long-wave radiation, the resonant interior response excited by an eastward-moving boundary has a cross-channel structure very different from that allowed by the corresponding linear model. This structure is oscillatory, i.e., radiating, near the northern boundary. For sufficiently high nonlinearity, the excited eddy will have closed recirculation regions and may detach from the boundary itself, propagating away from it like Gulf Stream rings.

Second, allowing for a slow time modulation of the northern boundary wave, in the weakly nonlinear case the resonant interior response obeys a time-dependent forced KdV equation. An initial condition corresponding to the previously-found steady equilibrium solution evolves, with soliton production in the region directly affected by the forcing. On the long time scale the interior response undergoes a nonlinear deterministic cascade process producing nonlinear radiation of shorter wavelength and permanent form, i.e., smaller nonlinear eddies.

Finally, in Section 4 the conclusions of the present study are given and directions for future research are discussed.

2. Free nonlinear radiation in the zonal channel

The model to be considered is the quasi-geostrophic, equivalent barotropic potential vorticity equation over variable relief in a zonal channel:

$$\nabla'^2\psi'_{t'} - \frac{1}{R^2}\psi'_{t'} + J'(\psi', \nabla'^2\psi' + f_0^* H') = 0, \quad (2.1)$$

where primed quantities are dimensional and subscripts indicate partial derivatives;

$$f_0^* = f_0 \frac{|\Delta d|}{H},$$

where f_0 is the (constant) Coriolis parameter; H is the average depth; $|\Delta d|$ the (small) depth variation around the mean value H; x is the along-channel (east–west) direction; y is the cross-channel (north–south) direction; ψ' is the velocity streamfunction;

$$\nabla'^2 = \frac{\partial^2}{\partial x'} + \frac{\partial^2}{\partial y'}$$

is the horizontal Laplacian;

$$J(a, b) = \frac{\partial a}{\partial x'}\frac{\partial b}{\partial y'} - \frac{\partial a}{\partial y'}\frac{\partial b}{\partial x'}$$

the Jacobian of (a, b);

$$R = \sqrt{g'H}/f_0$$

the Rossby deformation radius; and g' = reduced gravity.

The model (2.1) is scaled in a zonal channel of width L_1 according to

$$y' = L_1 y, \quad x' = L_2 x = (L_1/\delta_1)x.$$

Thus L_1, L_2 are the characteristic wavelengths of the motion in the y (cross-channel) and x (along-channel) directions, respectively, and $\delta_1 = L_1/L_2$ is their aspect ratio. Furthermore,

$$\left.\begin{aligned} t' &= Tt = (L_2/c')t = (L_1/\delta_1 c')t \\ \psi' &= \psi_0\psi = (UL_1)\psi \end{aligned}\right\},$$

where c' is a characteristic phase speed of the motion.

We consider a quasi-linear topography

$$f_0^* H'(y) = \beta y + \gamma h(y), \quad (2.2)$$

thus introducing an equivalent beta-effect.

With the above scaling the model (2.1) becomes

$$\frac{R^2}{L_1^2}\frac{\partial}{\partial t}(\psi_{yy} + \delta_1^2\psi_{xx}) - \psi_t + \frac{\beta R^2}{c'}\left[1 + \frac{\gamma L_1}{\beta}h_y(y)\right]\psi_x + \frac{\psi_0}{c'L_1}\frac{R^2}{L_1^2}J(\psi, \psi_{yy} + \delta_1^2\psi_{xx}) = 0. \quad (2.3)$$

The equivalent barotropic model (2.1) has two intrinsic length scales: the Rossby radius R and the north–south wavelength L_1. I shall consider parameter ranges with $L_1 \geqslant R$. Then, the scale for a typical phase speed is $c' = \beta R^2$ and the following dimensionless parameters are defined:

$$\delta_1^2 = L_1^2/L_2^2,$$

the already introduced aspect ratio of north–south (cross-channel) to east–west (axial) wavelengths;

$$\delta^2 = R^2/L_1^2,$$

the aspect ratio of the Rossby radius to north–south wavelength;

$$\epsilon = \gamma L_1/\beta,$$

the small parameter measuring the quasi-linearity of the relief; and

$$\mathrm{Ro} = \frac{\psi_0}{c'L_1}\frac{R^2}{{L_1}^2} = \frac{\psi_0}{\beta {L_1}^3} = \frac{U}{\beta {L_1}^2},$$

the β-Rossby number where U is the particle speed. Then, (2.3) becomes

$$\delta^2 \frac{\partial}{\partial t}(\psi_{yy} + {\delta_1}^2\psi_{xx}) - \psi_t + \psi_x + \epsilon h_y(y)\psi_x + \mathrm{Ro}J(\psi, \psi_{yy} + {\delta_1}^2\psi_{xx}) = 0. \quad (2.4)$$

Equation (2.4) allows for permanent-form nonlinear wave solutions. To derive them, we pass to the reference frame steadily translating with the wave, defined by

$$s = x - c\tau, \quad \tau = t,$$

where c is now the dimensionless phase speed. In this frame, (2.4) can be written as

$$J\left(\psi + \frac{c\delta^2}{\mathrm{Ro}}y, \{\mathrm{Ro}(\psi_{yy} + {\delta_1}^2\psi_{ss}) + y + \epsilon h(y) + cy\}\right) = 0$$

or

$$\mathrm{Ro}(\psi_{yy} + {\delta_1}^2\psi_{ss}) + y(1 + c) + \epsilon h(y) = F[\psi/(\delta^2 c/\mathrm{Ro}) + y]. \quad (2.5)$$

In other words, the potential vorticity is expressed as a functional F of the streamfunction in the moving frame. I shall consider only permanent wave solutions for which the functional F is analytic, thus excluding all modon-like solutions which are, however, admitted by (2.5) if F is taken to be multivalued (Larichev and Reznik, 1976; Flierl *et al.*, 1980). Looking for a solution localized in space and decaying at $x \to \pm\infty$ where there is no background flow, we obtain the shape of F:

$$F(Z) = (1 + c)Z + \epsilon h(Z)$$

everywhere. Thus (2.5) becomes

$$\delta^2(\psi_{yy} + {\delta_1}^2\psi_{ss}) = (1 + c)\frac{\psi}{c} + \epsilon\frac{\delta^2}{\mathrm{Ro}}\left\{h\left[\psi\Big/\left(\frac{\delta^2 c}{\mathrm{Ro}}\right) + y\right] - h(y)\right\}. \quad (2.6)$$

The nonlinear solutions are required to be of permanent form. Thus the weak nonlinearity must be balanced by a weak dispersion. Nonlinearity can be weak for two reasons: 1) Because the wave itself is weak (Ro $\ll$ 1). This corresponds to solutions having $U \ll c$, if U is the particle speed. Then particles will not be dynamically bound to the wave. 2) Because the functional is quasi-linear ($\epsilon \ll 1$). Then $U \geq c$ and particles can be bound to the wave which will have closed recirculation regions.

Nonlinearity balances dispersion if $\epsilon\mathrm{Ro}/\delta^2 = \delta^2{\delta_1}^2$. The most general parameter range in which this balance can be achieved is: $\epsilon = \delta^4 \ll 1$; $\mathrm{Ro} = {\delta_1}^2 \ll 1$. Then both 1) and 2) are true. From the definition of the dimensionless parameters, this corresponds to length scales $L_2 > L_1 > R$, the case of weak asymmetric nonlinear waves over weak relief. Permanent form solutions can then be found for (2.6), but these are not discussed here.

Two limiting cases are, however, of more interest. In the first case, condition 1) is relaxed. This is the limit ${\delta_1}^2 = \mathrm{Ro} \to 1$, in which the permanent wave becomes symmetric and has high amplitude: $U \geq c$. Topography is quasi-linear: $\epsilon = \delta^4 \ll 1$. The corresponding length scales are $L_2 = L_1 > R$. To solve (2.6) in the simplest example, I specialize to quadratic topography:

$$h(y) = y^2/2. \quad (2.7)$$

Then (2.6) becomes

$$\delta^2\nabla^2\psi = (1 + c)\frac{\psi}{c} + \delta^4 y\frac{\psi}{c} + \frac{\delta^2}{2}\left(\frac{\psi}{c}\right)^2. \quad (2.8)$$

Expanding in δ^2 we obtain

Zeroth-order

$$c_0 = -1,$$

Order δ^2

$$\nabla^2\psi_0 = -c_1\psi_0 + (\psi_0^2/2). \quad (2.8a)$$

Equation (2.8a) admits radially symmetric solutions analogous to those found by Flierl (1979b) with a mean shear flow. They were proposed as models for Gulf Stream rings, because their most important property is that they trap water in their cores. The radially symmetric solution of (2.8a) can be found numerically, imposing as boundary conditions

$$\psi_0|_{r=0} = A; \quad \left.\frac{d\psi_0}{dr}\right|_{r=0} = B; \quad \psi_0 \to 0 \quad \text{as} \quad r \to +\infty.$$

This uniquely determines the eigenvalue c_1 which is found to be a "reinforcement" to the westward linear phase speed $c_0 = -1$ ($= -\beta R^2$). In the reference frame ($\psi + cy$) this solution is shown in Fig. 1.

The second limit of interest occurs when relaxing condition (2), namely, the quasi-linearity of the topography. Then $\delta^2 \to 1$ and the related parameter range is defined by length scales $L_2 > L_1 = R$; ${\delta_1}^2 = \mathrm{Ro} < 1$ is the small parameter of the system and the wave amplitude is weak: $U < c$. We now keep the relief $h(y)$ general. Then (2.6) becomes, expanding $h[y + {\delta_1}^2(\psi/c)]$ in Taylor series at y,

$$\psi_{yy} + {\delta_1}^2\psi_{ss} = (1 + c)\frac{\psi}{c} + h_y\frac{\psi}{c} + {\delta_1}^2\frac{h_{yy}}{2}\left(\frac{\psi}{c}\right)^2. \quad (2.9)$$

Expanding ψ and c in terms of ${\delta_1}^2$,

$$\psi = \psi_0 + {\delta_1}^2\psi_1 + {\delta_1}^4\psi_2 + \cdots,$$

$$c = c_0 + {\delta_1}^2 c_1 + {\delta_1}^4 c_2 + \cdots.$$

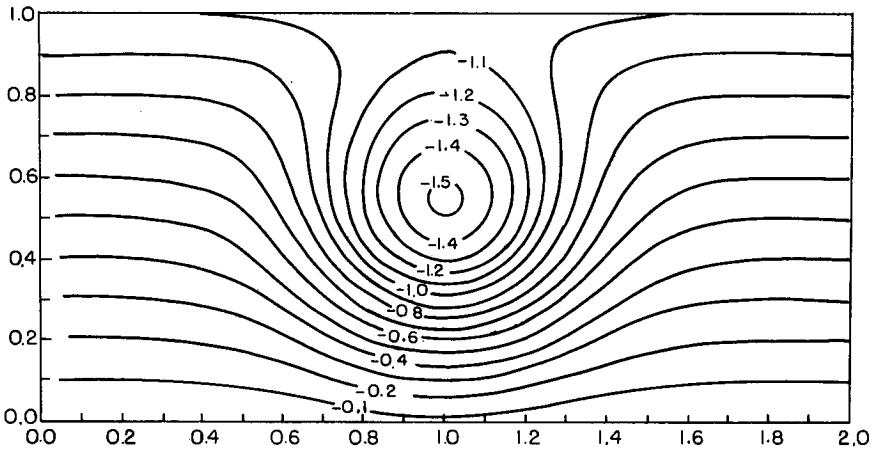

FIG. 1. Parameter range $L_2 = L_1 > R$; $\delta^2 \ll 1$, $\delta_1^2 = 1$. High amplitude monopole solution (2.8a), radially symmetric over quadratic relief $h(y) = y^2/2$ in the reference frame $(\psi_0 + c_0 y)$ with $c_0 = -1$.

We get:

Zeroth-order

$$\left.\begin{aligned} &\psi_0 = g(s)\phi(y) \\ &\phi_{yy} - \left(1 + \frac{1 + h_y}{c_0}\right)\phi = 0 \\ &\phi(0) = \phi(1) = 0 \end{aligned}\right\}. \qquad (2.9a)$$

This is a Sturm–Liouville problem. With zero or periodic boundary conditions at the channel walls, Sturm–Liouville theory insures the existence of an infinite denumerable set of orthogonal eigenfunctions ϕ_n and related eigenvalues c_{0n}. These are the equivalent of the phase speeds of linear Rossby waves over topography, dispersionless in the axial (x) direction. The $O(\delta_1^2)$ problem is

$$\psi_{1yy} - \left[1 + \frac{1 + h_y}{c_0}\right]\psi_1 = -\frac{c_1}{c_0^2}(1 + h_y)\psi_0 - \psi_{0ss} + \frac{h_{yy}}{2c_0^2}\psi_0^2. \qquad (2.9b)$$

The solvability condition for ψ_1 implies multiplying (2.9b) through $\phi(y)$, one of the eigensolutions of (2.9a), and integrating over the channel width. This gives the equation for $g(s)$,

$$a_1 g_{ss} + \frac{c_1}{c_0^2} a_2 g - \frac{a_3}{2c_0^2} g^2 = 0, \qquad (2.10)$$

with

$$\left.\begin{aligned} a_1 &= \int_0^1 \phi^2 dy \\ a_2 &= \int_0^1 \phi^2(1 + h_y)dy \\ a_3 &= \int_0^1 h_{yy}\phi^3 dy \end{aligned}\right\}. \qquad (2.10a)$$

Eq. (2.10) is the KdV equation. The permanent wave solution decaying to $s \to \pm\infty$ is the solitary wave

$$g(s) = A\,\mathrm{sech}^2(Bs). \qquad (2.11)$$

Values of A, B and c_1 are obtained by substituting (2.11) into (2.10):

$$A = -\frac{12c_0^2 a_1}{a_3} B^2, \qquad (2.12a)$$

$$c_1 = -\frac{4a_1 c_0^2}{a_2} B^2. \qquad (2.12b)$$

Equation (2.11) is a one-parameter family of solutions, depending upon the value assigned to B. Also, as evident from (2.12a), the solution (2.11) is an "elevation" ($A > 0$) or "depression" ($A < 0$) solitary wave according to $a_1/a_3 \lesseqgtr 0$. These solutions are analogous to those found by Malanotte-Rizzoli (1980a,b) for the barotropic, quasi-geostrophic vorticity equation over variable relief, for which the sinusoidal topography $h(y) = \sin y + \sin(2y)$ was used. They also have a weak amplitude. However, it can be shown that the Rossby number can be numerically increased and the limit of high amplitude ($U \gtrsim c$) can be reached. The numerical experiments of Malanotte-Rizzoli (1980b) demonstrated that the solitary wave solutions maintain their property of permanent shape even in the limit $\mathrm{Ro} \to 1$, beyond the validity range of the analytical theory.

3. Equilibrium boundary-forced solutions

The problem of the existence of boundary-forced nonlinear wave solutions, when the forcing is imposed at the northern wall of the zonal channel, is now addressed. The northern wall boundary condition can be thought of as a crude idealization of a time-dependent northern current.

Model (2.1) is nondimensionalized as in Section 2. The equilibrium-forced radiation of (2.1) in the parameter range $\delta^2 \equiv 1$; $\delta_1^2 \ll 1$, corresponding to the second case explored in Section 2, is studied in detail. A completely analogous treatment can be repeated for the very weakly nonlinear case $\delta^2 \ll 1$; $\delta_1^2 \ll 1$. The opposite case of strongly nonlinear, symmetric eddies with $\delta_1^2 = 1$, $\delta^2 \ll 1$ (first case treated in Section 2), cannot be treated with the following asymptotic treatment. It can be thought of, however, as the limit of either of the above problems when increasing simultaneously the strength and symmetry of the solution. This limit can be reached numerically.

With $\delta^2 = 1$, $\mathrm{Ro} = \delta_1^2$, and keeping the model in time-dependent form, (2.1) is

$$\psi_{yyt} - \psi_t + \psi_x + h_y\psi_x + \delta_1^2[\psi_{xxt} + J(\psi, \psi_{yy})] + \delta_1^4 J(\psi, \psi_{xx}) = 0. \quad (3.1)$$

We impose at the northern wall a traveling wave forcing

$$\psi(x, 1, t) = f_b(x, t) = f_b(x - c_b t). \quad (3.2a)$$

The equilibrium-forced solution, if it exists, will have a phase speed c fixed by the boundary driving:

$$c = c_b. \quad (3.2b)$$

Thus, we seek a steady forced solution of the form

$$\psi = \psi(x - ct).$$

We pass to the reference frame $s = x - ct$ in which the wave is steady. Following the procedure of Section 2, we expand ψ and c_b in power series of the small parameter δ_1^2. The zero-order problem is identical to (2.9a), with $\psi_0 = g(s)\phi(y)$. The $O(\delta_1^2)$ problem is now

$$\psi_{1yys} - \left[1 + \frac{1 + h_y}{c_0}\right]\psi_{1s} = -\frac{c_1(1 + h_y)}{c_0^2}\psi_{0s} - \psi_{0sss} + \frac{h_{yy}}{c_0^2}\psi_0\psi_{0s}, \quad (3.3)$$

with boundary conditions

$$\left.\begin{aligned}\psi(s, 0) &= 0 \quad \text{at} \quad y = 0\\ \psi(s, 1) &= f_b(s) \quad \text{at} \quad y = 1\end{aligned}\right\}. \quad (3.4)$$

Notice that in the free case, repeating for (3.3) the treatment of Section 2, not only the solitary wave solution (2.11) but also periodic cnoidal wave solutions would be obtained. (See Malanotte-Rizzoli, 1982, for a review of the solutions of the KdV equation.) These were not allowed by (2.9b) because of the requirement, made at the beginning of Section 2, for the solution to be localized in space. This requirement is not made here. There are two choices to satisfy the boundary condition (3.4). In the first case, consider a boundary forcing of O(1). Then (3.4) is

$$\left.\begin{aligned}\psi_0(s, 0) &= 0 \quad \text{at} \quad y = 0\\ \psi_0(s, 1) &= f_b(s) \quad \text{at} \quad y = 1\end{aligned}\right\}. \quad (3.5)$$

The equilibrium-forced solution is found at zero-order and is given by

$$\left.\begin{aligned}\psi_0 &= g(s)\phi(y)\\ g(s) &= f_b(s)\end{aligned}\right\}, \quad (3.5a)$$

$$\left.\begin{aligned}\phi_{yy} - \left[1 + \frac{1 + h_y}{c_0}\right]\phi &= 0\\ \phi(0) = 0, \quad \phi(1) &= 1\end{aligned}\right\}. \quad (3.5b)$$

In general, the solution to (3.5b) is:

$$\phi = \phi(\bar{K}y)/\phi(\bar{K}), \quad (3.6)$$

where we define $\bar{K}$ as the average y-wavenumber. Equation (3.6) is valid for all the values of $c_0 \gtrless 0$ which do not satisfy $\phi(\bar{K}) \equiv 0$, that is, the eigenfrequencies c_{0n} of the free modes in the zonal channel. If $c_0 \equiv c_{0n}$, the forced response is infinite, because system (3.5) is simply the linear oscillator problem forced at one of its resonant frequencies.

The most interesting case, however, is just when $c \equiv c_{0n}$, one of the resonant eigenfrequencies. If $f_b = O(1)$, the weakly nonlinear oscillator will obviously respond in the same way as the purely linear oscillator, as shown by (3.5) and (3.6). Consider then the weak forcing case, $f_b = O(\delta_1^2)$. The zero-order problem is now solved by

$$\psi_{0n} = g_n(s)\phi_n(y), \quad \psi_{0n}(s, 0) = \psi_{0n}(s, 1) \equiv 0, \quad (3.7a)$$

with $\phi \equiv \phi_n$ and $c_0 \equiv c_{0n}$ solutions of (2.9a). The $O(\delta_1^2)$ problem now is

$$\psi_{1yys} - \left[1 + \frac{1 + h_y}{c_0}\right]\psi_{1s} = -\frac{c_1(1 + h_y)}{c_0^2}\psi_{0s} - \psi_{0sss} + \frac{h_{yy}}{c_0^2}\psi_0\psi_{0s},$$
$$\psi_1(s, 0) = 0,$$
$$\psi_1(s, 1) = f_b(s). \quad (3.7b)$$

In the present nonlinear case, a weak forcing of $O(\delta_1^2)$ at one of the resonant frequencies c_{0n} excites a finite response of O(1).

The usual solvability condition applied to (3.7) gives the equation for $g_n(s)$:

$$a_1 g_{nsss} + \frac{c_{1n}}{c_{0n}^2} a_2 g_{ns} - \frac{a_3}{c_{0n}^2} g_n g_{ns} = \alpha f_{bs} \quad (3.8)$$

or

$$a_1 g_{nss} + \frac{c_{1n}}{c_{0n}^2} a_2 g_n - \frac{a_3}{2c_{0n}^2} g_n^2 = \alpha f_b + K, \quad (3.8a)$$

with K an integration constant,

$$\alpha = \phi_{ny}|_{y=1}, \quad (3.8b)$$

and a_1, a_2 and a_3 are given by (2.10a). Equation (3.8) is the inhomogeneous form of the KdV equation. For

a general forcing f_b, the solutions of (3.8) can be found numerically.

We can solve (3.8a) analytically for the specific case

$$f_b = a_b \operatorname{sech}^4(Bs), \quad K \equiv 0, \tag{3.9}$$

by seeking a solution of the same shape as the free nonlinear wave

$$g_n = A \operatorname{sech}^2(Bs), \tag{3.10}$$

and for the particular case when the $O(\delta_1^2)$ boundary phase speed

$$c_1 = -\frac{4a_1c_0^2}{a_2} B_2 = c_1^*, \tag{3.11}$$

that is, the $O(\delta_1^2)$ phase speed of the free nonlinear wave.

In the forced case the amplitude of the response is fixed by the forcing wavenumber B and amplitude a_b. Specifically, it must satisfy

$$A^2 + \frac{12c_0^2B^2a_1}{a_3} A + \frac{2\alpha c_0^2}{a_3} a_b = 0. \tag{3.12}$$

Equation (3.12) shows that multiple equilibrium responses exist if

$$\left(\frac{6c_0^2B^2a_1}{a_3}\right)^2 > \frac{2\alpha c_0^2 a_b}{a_3}. \tag{3.12a}$$

Equation (3.12a) is a constraint on the possible wavelengths $1/B$, once the forcing amplitude a_b is given. The multiple response curve (3.12a) is shown in Fig. 2 for the two cases $a_3 \gtrless 0$.

Let us consider the expression (3.11) for $c_1 = c_1^*$. For those reliefs $h(y)$ for which $a_2 > 0$ (as for a quadratic topography $h = y^2/2$), as $a_1 > 0$ always, $c_1^* < 0$. Equation (3.12) can equivalently be written as

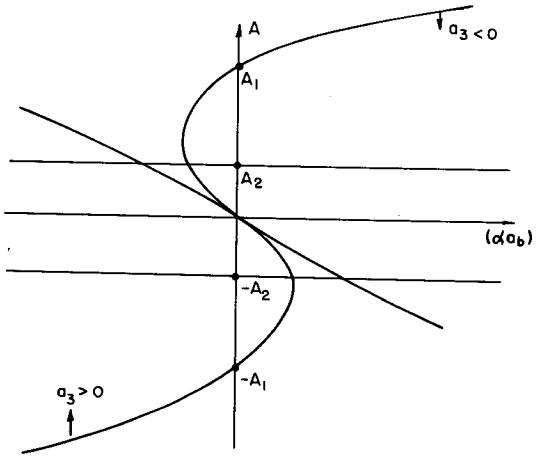

FIG. 2. Multiple response curve (3.12) for the amplitude A of the resonantly excited equilibrium response $g = A \operatorname{sech}^2(Bs)$ with the boundary forcing $f_b = a_b \operatorname{sech}^4(Bs)$. The response amplitude A is given as a function of the forcing amplitude (αa_b) for the two cases $a_3 \gtrless 0$, with a_3 defined by (2.10a).

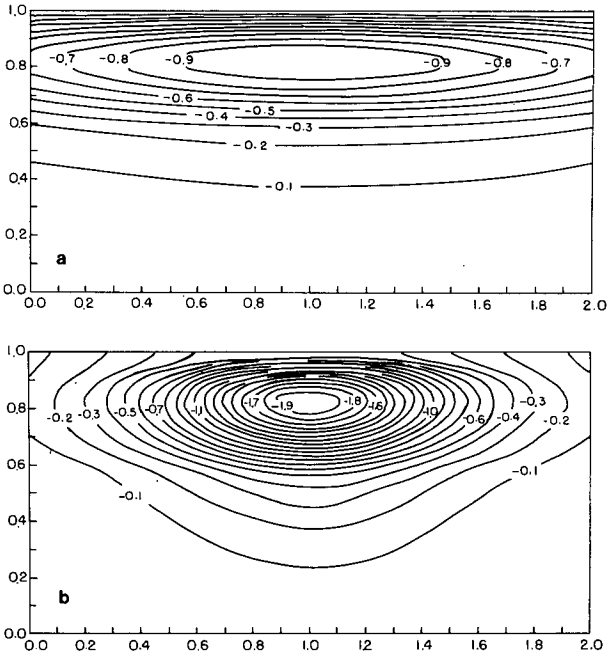

FIG. 3. Resonantly excited equilibrium nonlinear waves with a boundary forcing $f_b = \operatorname{sech}^4(Bs)$ and $a_b = 1$ over the relief $h(y) = -2.2y + 2.2y^2$. (a) Lowest westward-propagating wave $\psi_0 = A \operatorname{sech}^2(Bs)\phi_{1W}(y)$, where $B = 0.7$, $A \approx -1$, and $\delta_1^2 \approx 0.1$. (b) Lowest westward-propagating wave $\psi = \psi_0 + \delta_1^2\psi_1$, with ψ_0 as in (a). $B = 2$, $A = -2$ and $\mathrm{Ro} = \delta_1^2 \sim 1$.

$$A^2 - \frac{3a_2}{a_3} c_1 A + \frac{2c_0^2(\alpha a_b)}{a_3} = 0$$

or

$$A = -\frac{1}{2}\frac{3a_2}{a_3}(-c_1) \pm \left[\frac{1}{4}\left(\frac{3a_2(-c_1)}{a_3}\right)^2 - \frac{2c_0^2(\alpha a_b)}{a_3}\right]^{1/2}. \tag{3.12b}$$

If $a_3 < 0$ and $\alpha a_b > 0$, there are two equilibrium forced solutions, one with $A_1 > 0$ and the other with $A_2 < 0$. If $\alpha a_b < 0$ there are again two equilibrium forced solutions, both with $A > 0$, if

$$(\alpha a_b) > -\frac{1}{4}\left(\frac{3a_2(-c_1)}{a_3}\right)^2 \frac{(-a_3)}{2c_0^2} = -\frac{(-a_3)}{2c_0^2}\left(\frac{6a_1c_0^2B^2}{a_3}\right)^2 = (\alpha a_b)_{\min},$$

which is always satisfied.

If $a_3 > 0$, for $(\alpha a_b) < 0$ the two equilibrium responses have $A_1 > 0$, $A_2 < 0$; for $0 < \alpha a_b < (\alpha a_b)_{\max}$ they both have $A < 0$. Thus, the two equilibrium responses always exist.

With a boundary forcing $f_b = \operatorname{sech}^4(Bs)$, consider the weakly nonlinear case $\delta_1^2 \approx 10^{-1}$. In Fig. 3a we show the equilibrium solution ψ_0 with $c_0 = c_{01} \approx -\frac{1}{6} < 0$, the lowest westward-propagating eigenmode over $h(y) = -2.2y + 2.2y^2$. With the above

aspect ratio, we have for this mode $B = 0.7$; $c_1 \approx +1/3 > 0$ as evaluated from (3.11); $\phi_y|_{y=1} < 0$, $\alpha a_b < 0$; and $a_3 > 0$. We display the solution with $A < 0$, specifically $A \approx -1$ as evaluated from (3.12b). The pattern of Fig. 3a is only the zero-order resonant equilibrium response ψ_0. The full solution of the problem to $O(\delta_1^2)$ is $\psi_0 + \delta_1^2\psi_1$. In Fig. 3b we show the pattern of $(\psi_0 + \delta_1^2\psi_1)$, again for the lowest westward-propagating eigenmode of Fig. 3a, but in the limit $\mathrm{Ro} = \delta_1^2 \to 1$. In Fig. 3b, $A = -2$ and $B = 2$. From Fig. 3b it is clear that the equilibrium resonant response $(\psi_0 + \delta_1^2\psi_1)$ is radiating away from the northern boundary. Even though the limit $\mathrm{Ro} = \delta_1^2 \to 1$ is outside the validity range of the analytical treatment, Fig. 3b is shown to emphasize the similarity of these resonant nonlinear eddy patterns with the eddies shed by unstable jets in numerical experiments (Holland, 1978; Ikeda and Apel, 1981; Ikeda, 1981). This similarity is obviously more striking going to the (numerical) limit of high nonlinearity (high aspect ratio) but it is true also for the weakly nonlinear case. In fact, the eddy shapes excited in the numerical experiments quoted above are often highly elongated and asymmetric.

I have examined the details of the equilibrium resonant solution under the forcing $f_b = a_b \operatorname{sech}^4(Bs)$ when $c_1 \equiv c_1^*$ as given by (3.11). Let us examine the behavior of the resonant response for an arbitrary value of the phase speed c_1, under the same northern forcing. Then, with $K = 0$, (3.8a) is

$$a_1 g_{ss} + \frac{c_1}{{c_0}^2} a_2 g - \frac{a_3}{2{c_0}^2} g^2 = \alpha a_b \operatorname{sech}^4(Bs), \quad (3.13)$$

where we have dropped the subscript n for simplicity.

For arbitrary c_1, the solution of (3.13) will not be the simple function $\operatorname{sech}^2(Bs)$. First, from (3.13), $g \neq 0$ always. In the limit $c_1 \to \pm\infty$, the asymptotic solution of (3.13) is

$$g(s) = \frac{(\alpha a_b){c_0}^2}{a_2 c_1} \operatorname{sech}^4(Bs), \quad (3.14a)$$

that is, the solution tends asymptotically to zero. If $c_1 \to \infty$, $g \to \infty$, the asymptotic behavior is given by

$$g = (2a_2/a_3)c_1, \quad (3.14b)$$

a straight line in c_1. The limit $c_1 \to 0$ leads to

$$a_1 g_{ss} - \frac{a_3}{2{c_0}^2} g^2 = \alpha a_b \operatorname{sech}^4(Bs), \quad (3.14c)$$

which is not amenable to a simple analytic solution. However, the forcing function is even around $s = 0$. A Taylor series expansion of (3.14c) can be performed around $s = 0$. This leads to

$$g_s|_{s=0} = g_{sss}|_{s=0} \cdots \equiv 0,$$

$$g_{ss}|_{s=0} = \frac{4(\alpha a_b)B^2{c_0}^2}{a_3 g},$$

$$a_1 g_{ss}|_{s=0} - \frac{a_3}{2{c_0}^2} g^2|_{s=0} = \alpha a_b.$$

As $g_{ss} \propto 1/g$, unless $(\alpha a_b) \to 0$, the balance in the third of the above relationships is essentially $-a_3/2{c_0}^2 g^2 \approx \alpha a_b$. If $(\alpha a_b) \to 0$, we recover the limit of the free nonlinear solution. Then, for $c_1 \to 0$, near $s = 0$

$$g \approx \pm\left(\frac{-2(\alpha a_b){c_0}^2}{a_3}\right)^{1/2}. \quad (3.14d)$$

The solution is known when $c_1 = c_1^* < 0$.

From the above limits, the behavior of the solution can be inferred as a function of c_1, if with A we now indicate its maximum amplitude. Distinguish the following cases, considering topographies for which $a_2 > 0$:

a) $a_3 < 0$.

a1) $\alpha a_b > 0$.

From Fig. 2, at $c_1 = c_1^*$ two solutions exist, with $A_1 < 0$, $A_2 > 0$. From (3.14a): $\lim_{c_1 \to \pm\infty} g(s) = \pm 0$. From (3.14b): $\lim_{c_1 \to \pm\infty} g(s) = \mp\infty$. From (3.14d), when $c_1 \to 0$, near $s = 0$, g has two real solutions, one positive and the other negative. Through continuity, two real solutions can be inferred to exist for every s. The above information can be summarized in the plot of Fig. 4a (upper panel).

a2) $\alpha a_b < 0$.

From Fig. 2, at $c_1 = c_1^*$ two solutions exist, both with $A > 0$. From (3.14a): $\lim_{c_1 \to \pm\infty} g(s) = \mp 0$. From (3.14b): $\lim_{c_1 \to \pm\infty} g(s) = \mp\infty$. From (3.14d); however, in this case no real solutions exist for $c_1 \to 0$ near $s = 0$. The solutions are purely imaginary. Thus there will be a region around $c_1 \to 0$ in which no real solution exists. The lower panel of Fig. 4a shows the above behavior. In this case, no real solution exists when $c_1 \to 0$, say for $c_1^{(1)} < c_1 < c_1^{(2)}$.

The corresponding two further cases:

b1) $a_3 > 0$; $\alpha a_b > 0$,

b2) $a_3 > 0$; $\alpha a_b < 0$,

are shown in the upper and lower panels, respectively, of Fig. 4b. From Figs. 4a and b we can conclude that either two equilibrium resonant responses always exist for arbitrary c_1, or that no real solutions exist near $c_1 \to 0$. The generalization to an arbitrary forcing function f_b can be carried out only by solving (3.8a) numerically. The possibility of a nonlinear resonance cannot be excluded by the above specialized treatment. However, as (3.8a) is a quadratic equation in the response amplitude, it may be inferred that in the general case also, no more than two equilibrium steady responses will be possible.

We have thus far considered the weak amplitude limit of asymmetric radiation in the zonal channel. Let us focus again on the zero-order linear problem (2.9a), always for a forcing function f_b moving at one of the resonant eigenfrequencies $c_0 \equiv c_{0n}$ of (2.9a).

Over reliefs for which $h_y > 0$ everywhere, like

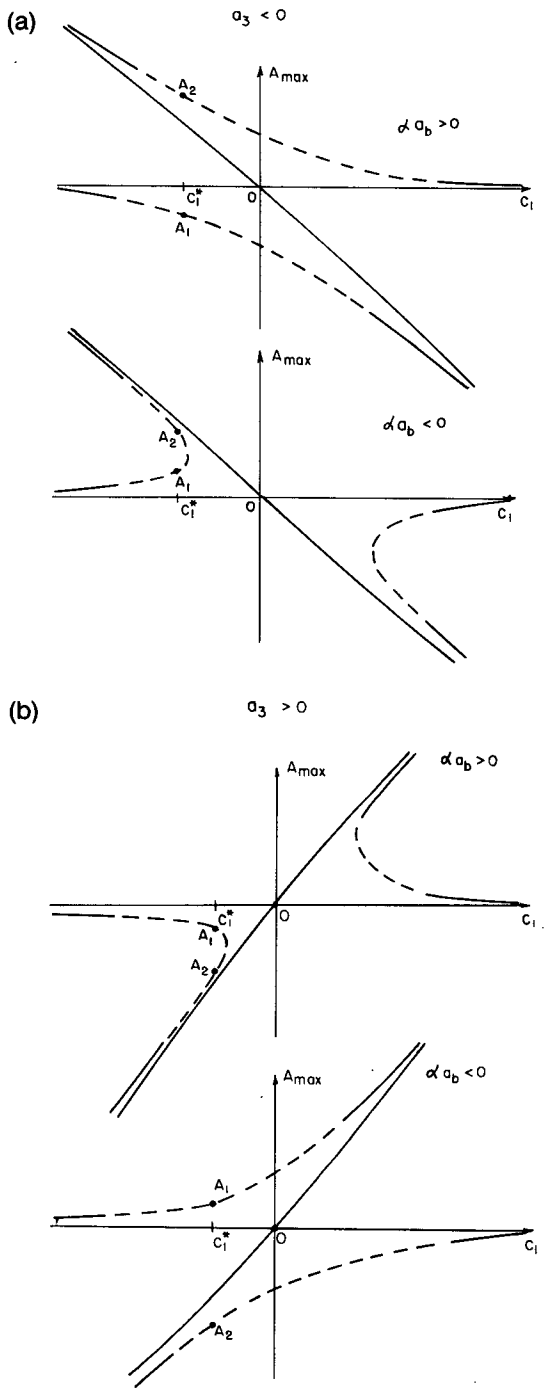

FIG. 4. Multiple response curve (3.13) for the maximum amplitude A_{max} of the resonant equilibrium solution $g(s)$ as a function of the nonlinear phase speed c_1. (a) Case $a_3 < 0$ with a_3 defined by (2.10a); $\alpha a_b > 0$ (upper panel) and $\alpha a_b < 0$ (lower panel). (b) Case $a_3 > 0$; $\alpha a_b > 0$ (upper panel) and $\alpha a_b < 0$ (lower panel).

$h = y^2/2$, a northward-sloping topography, the only solutions to (2.9a) have a westward zero-order phase speed. Thus, only a westward-moving northern boundary will excite interior resonant responses capable of radiating. Let us choose the topography $h = -2.2y + 3y^2$, again sloping northward, but for which h_y changes sign in the zonal channel. Such a relief is shown in Fig. 5a, and allows for eastward-propagating eigenmodes. However, the relief being very similar to the purely northward-sloping case, the eastward-propagating eigenmodes have a weakly oscillatory behavior, confined to an interior region of the basin and decaying away from it. Figure 5b shows the lowest eigenmode with $c_{01} > 0$ for such a relief. This is not surprising because, for weak nonlinearity, the zeroth-order problem gives a y-structure identical to the linear problem, and a relief which is mostly northward sloping acts essentially as an intensified β-effect.

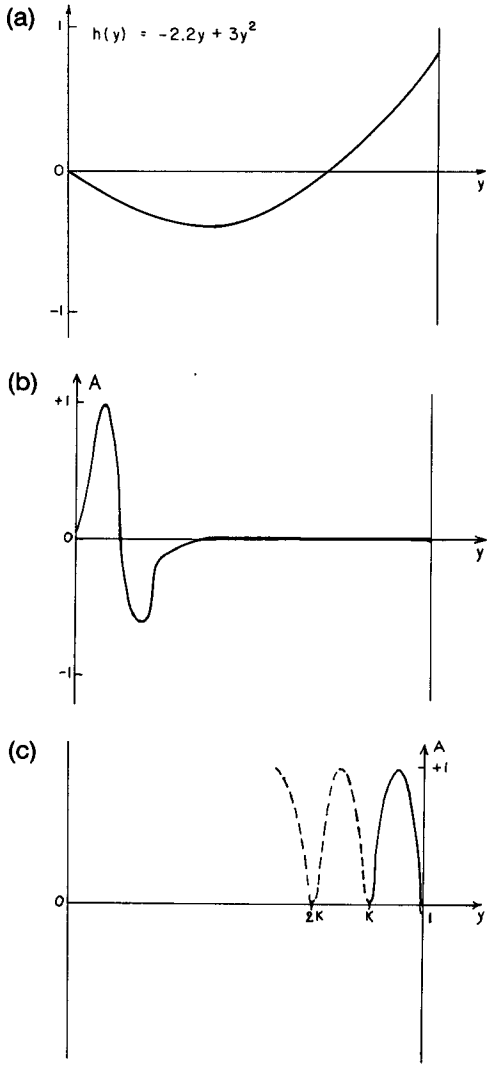

FIG. 5. (a) Shape of the relief $h(y) = -2.2y + 3y^2$ in the zonal channel $0 \leq y \leq 1$. (b) Lowest eigenmode over the relief of (a), eastward propagating for the linear or weakly nonlinear problem. (c) Structure of the solution near the northern wall in the highly nonlinear case Ro $\rightarrow$ 1 over general topography, and in particular over a quadratic relief of the type shown in (a).

Let us now increase the amplitude of the forcing at the northern wall. We want the nonlinear resonant response to be long-wave radiation in the zonal channel, with a wavelength aspect ratio $\delta_1 \ll 1$ but with a Rossby number Ro $\to$ 1. We consider therefore the limit of a boundary forcing f_b = O(1) at one of the resonant frequencies c_{0n}, which will excite a response ψ_0 = O($1/\delta_1^2$). Then, rescaling problem (3.1) and putting $\psi^* = (1/\delta_1^2)\psi$, (3.3) becomes

$$\frac{1}{\delta_1^2}[-c\psi^*_{yys} + c\psi^*_s + \psi^*_s + h_y\psi^*_s + J(\psi^*, \psi^*_{yy})] - c\psi^*_{sss} + J(\psi^*, \psi^*_{ss}) = 0. \quad (3.15)$$

The lowest order ($1/\delta_1^2$) is now

$$\psi^*_{0yys} - \left[1 + \frac{1 + h_y}{c_0}\right]\psi^*_{0s} - \frac{1}{c_0}(\psi^*_{0s}\psi^*_{0yyy} - \psi^*_{0y}\psi^*_{0yys}) = 0. \quad (3.16)$$

Equation (3.16) is a nonlinear eigenvalue problem whose eigenfunctions and eigenvalues c_{0n}, if they exist, will be very different from those of (3.6a).

We can think of approaching (3.16) in two ways. First, start from (3.7a) and force with a boundary wave f_b of gradually increasing amplitude and speed c_{0n}. The study of (3.16) with $c_0 = c_{0n}$ assigned will then allow us to infer the properties of the resonant response in the limit $f_b \to 1$.

Alternatively, we can study (3.16) directly as the zero-order problem, with $\psi_0 = 0$ at $y = 0$, 1, and see whether solutions with oscillatory behavior which are also eastward moving with $c_0 > 0$, do exist.

The behavior of (3.16) is explored near the northern boundary $y = 1$. First we pass to the coordinate $y' = y - 1$, for which (3.16) remains formally identical. We then transform (3.16) into an equivalent nonlinear problem, the approximate expression of which, valid near the northern boundary $y' = 0$, is (see the Appendix)

$$\psi^*_{\delta y'y'} + [(1 + c_0)y' + h(y')][1 - \exp(\psi^*_\delta/c_0y')] - \psi^*_\delta + [y' + h(y')] = 0, \quad (3.17)$$

with boundary condition $\psi^*_\delta(s, 0) = 0$ at $y' = 0$. Equation (3.17) is valid near $y' = 0$. We can further approximate it by expanding $\exp(\psi^*_\delta/c_0y')$ in a Taylor series of ψ^*_δ as $\psi^*_\delta \to 0$ at $y' = 0$. Retaining terms to O(ψ^{*2}_δ), (3.17) becomes

$$\psi^*_{\delta y'y'} - \frac{(1 + 2c_0)y' + h(y')}{c_0y'}\psi^*_\delta - \frac{(1 + c_0)y' + h(y')}{2c_0^2y'^2} \times \psi^{*2}_\delta + [y' + h(y')] = 0. \quad (3.18)$$

Equation (3.18) is a KdV equation with variable coefficients, valid in a layer near the northern boundary where the coefficients are gradually varying functions of y'. It is thus equivalent to the KdV equation governing the propagation of cnoidal and solitary waves in a channel of gradually varying depth and width (Miles, 1979). Because (3.18) is not separable in (s, y'), the general shape of the solution locally in s will be the equivalent of the solution for the gradually varying channel, that is,

$$\psi^*_\delta = A(s, y')cn^2\left[\frac{B(s, y')}{n(s)}y' + \delta(s, y')\right], \quad (3.19)$$

where $n(s)$ is the modulus of the Jacobian elliptic function cn and $0 \leq n \leq 1$. The solution will thus have the shape of a cnoidal wave, oscillatory in cross-channel direction, with values for A, B and δ slowly varying in y'. Also, the amplitude A, wavelength $B(s, y')/n(s)$ and phase $\delta(s, y')$ undergo a modulation during the propagation along the channel. The boundary condition $\psi^*_\delta = 0$ at $y' = 0$ is equivalent to quantizing, locally in s, the reference phase $\delta(s, 0)$ at the northern wall, and assigning a boundary value to it:

$$\delta(s, 0) = (2l + 1)\bar{K}(s, 0) \quad \text{with} \quad l = 0, 1, 2, \ldots.$$

$\bar{K}(s, 0)$ is the value at $y' = 0$ of the related Jacobian elliptic integral. This is consistent with the solution for the cnoidal or solitary wave in the gradually varying channel (Miles, 1979) in which the reference phase is evaluated relative to a reference point.

Equation (3.19) shows that the y-structure of the solution near the northern wall is now very different from that of the weakly nonlinear case. This oscillatory structure is modulated by the amplitude $A(s, y')$; $A(s, y')$, $B(s, y')$ and $\delta(s, y')$ can be found by substituting (3.19) into (3.18). This yields

$$A^2(s, y') = \frac{6n(s)}{1 - n(s)}\frac{c_0^2y'^2}{(1 + c_0)y' + h(y')}[y' + h(y')], \quad (3.19a)$$

showing that the solution does not decay away from the northern boundary. Equation (3.19a) also shows that the solutions exist for all the reliefs for which $h(y') > 0$ and $h(0) \sim$ O(1). In fact, (3.19a) can be written in this case as

$$A^2 \approx \frac{6n(s)}{1 - n(s)}c_0^2y'^2, \quad (3.19b)$$

neglecting y' with respect to $h(y') \sim$ O(1). This is true for the specific case

$$h = \frac{y^2}{2} = \frac{(y' + 1)^2}{2},$$

a purely northward-sloping relief, and in the previously considered case, $h(y) = -2.2y + 3y^2$.

For this type of relief, (3.19b) also shows that the solution exists for both $c_0 \gtrless 0$, that is, also in the case in which the boundary wave is eastward propagating. Figure 5c shows the qualitative structure of (3.19) near

the northern boundary, and must be compared with Fig. 5b, the solution in the weakly nonlinear case. The above results indicate how the limit of high nonlinearity may profoundly modify the interior field response and allow for radiating interior responses even when the northern boundary is eastward moving.

A second effect of nonlinearity can be investigated for the weakly nonlinear system (3.1). Consider again a weak boundary forcing $f_b = O(\delta_1^2)$ at one of the resonant eigenfrequencies c_{0n} of the zero-order problem (2.9a). Let the $O(\delta_1^2)$ phase speed of the forcing wave—the detuning from the linear speed c_0—be a slowly varying function of a long time scale T. The boundary wave is moving at the constant zero-order speed c_0 with a slow modulation

$$f_b = f_b(s, T) = f_b(x - c_0 t, T) \tag{3.20}$$

with $T = \delta_1^2 t$. Introducing the long time scale T, system (3.1) becomes

$$\psi_{yyt} + \delta_1^2\psi_{yyT} - \psi_t - \delta_1^2\psi_T + \psi_x + h_y\psi_x + \delta_1^2[\psi_{xxt} + J(\psi, \psi_{yy})] + \delta_1^4\psi_{xxT} + \delta_1^4 J(\psi, \psi_{xx}) = 0. \tag{3.21}$$

Passing again to the moving frame $s = x - c_0 t$ and expanding ψ_0 in powers of δ_1^2, the zero order system is the same:

$$\psi_{0yys} - \left[1 + \frac{1 + h_y}{c_0}\right]\psi_{0s} = 0, \tag{3.22a}$$

where now $\psi_0 = g(s, T)\phi(y)$ and $\phi(0) = 0$, and $\phi(1) = 0$. The $O(\delta_1^2)$ system becomes

$$\psi_{1yys} - \left[1 + \frac{1 + h_y}{c_0}\right]\psi_{1s} = \frac{1 + h_y}{c_0^2}\phi g_T - \phi g_{sss} + \frac{1}{c_0^2} h_{yy}\phi^2 g g_s \tag{3.22b}$$

with $\psi_1(s, 0) = 0$; $\psi_1(s, 1) = f_b(s)$. Multiplying again through by ϕ, integrating across the channel and applying the boundary condition on ψ_1 at $y = 1$, gives

$$g_T + \frac{a_3}{a_2} g g_s - \frac{a_1 c_0^2}{a_2} g_{sss} = -\frac{\alpha c_0^2}{a_2} f_{bs}, \tag{3.23}$$

where $\alpha = \phi_y|_{y=1}$, and a_1, a_2 and a_3 are given by (3.8b). Equation (3.23) is the time-dependent version of the forced KdV equation. Notice that, had we not allowed for a slow time evolution of the $O(\delta_1^2)$ phase speed c_1, but instead kept it constant, we would again obtain the resonant equilibrium equation (3.8).

Equation (3.23) can be solved numerically by choosing a specific shape for the forcing function f_b. Choose $f_b = a_b \operatorname{sech}^4(Bs)$, for which, in the steady equilibrium case, the solution is $g = A \operatorname{sech}^2(Bs)$. Rescale s through $s = a_3/a_2\zeta$. Equation (3.23) becomes

$$g_T + g g_\zeta - \frac{a_1 a_2^2 c_0^2}{a_3^3} g_{\zeta\zeta\zeta} = -\frac{\alpha c_0^2}{a_3} f_{b\zeta}. \tag{3.24}$$

The unforced version of (3.24) is the canonical form of the time-dependent KdV equation (Jeffrey and Kakutani, 1972; Zabusky and Kruskal, 1965). To solve it, a spectral numerical code based upon Fourier decomposition has been developed, following Fornberg and Whitham (1978) in a channel with $0 \leq y \leq 1$ and $0 \leq x \leq 8$, with periodic boundary conditions in x.

Equation (3.24) has been solved for the lowest westward-propagating mode of $h(y) = -2.2y + 2.2y^2$, shown in Fig. 3a. For this mode, $c_0 \sim -\frac{1}{6}$ and $c_1 \sim \frac{1}{3}$ in the steady equilibrium case. Evaluating a_1, a_2 and a_3 for this mode as in (2.10a), the dispersion coefficient is

$$\sqrt{\mu} = \left(\left|\frac{a_1 c_0^2 a_2^2}{a_3^3}\right|\right)^{1/2} \sim \frac{10^{-1}}{\sqrt{12}}.$$

With the chosen forcing function $f_b = a_b \operatorname{sech}^4(B\zeta)$, the right-hand side of (3.24) becomes

$$\frac{-\alpha c_0^2}{a_3} f_b = \frac{4\alpha c_0^2}{a_3} a_b B \operatorname{sech}^4(B\zeta)\tanh(B\zeta).$$

For the chosen mode $a_3 > 0$ and $\alpha < 0$. Choosing the wavenumber of the forcing wave to be $B = 1$, we have

$$\frac{4\alpha c_0^2}{a_3} B a_b \approx 2a_b.$$

Equation (3.24) has been solved for the two specific values of the forcing amplitude a_b: 1) $a_b = -0.005$; 2) $a_b = -0.025$. In both cases, $(\alpha a_b) > 0$. From Fig. 2, on the multiple response curve with $a_3 > 0$, for $(\alpha a_b) > 0$ two possible response amplitudes are allowed in the steady case, both negative, i.e., $A < 0$. With the above values for a_b, α, c_0, a_1, a_2 and a_3, the values of A can be evaluated from (3.12). With the initial condition $g(0, \zeta) = A \operatorname{sech}^2(B\zeta)$, the numerical integration of (3.24) for the cases 1) and 2) shows a completely analogous evolution of the given initial condition on the long time scale T, but it is slower for case 1) because the forcing amplitude a_b is weaker. Thus, we present results relative to case 2) only. For this case, the two equilibrium amplitudes obtained from (3.12) are $A_1 \approx -0.03$ and $A_2 \approx -1$; we choose $A = A_2 \approx -1$. Notice that the corresponding free nonlinear wave amplitude as given by (2.12a) is in this case $A_{\text{free}} \approx -0.4$, which is also negative.

In Fig. 6 the forcing function

$$(4\alpha c_0^2/a_3)Ba_b \operatorname{sech}^4(B\zeta)\tanh(B\zeta) \approx -0.05 \operatorname{sech}^4(B\zeta)\tanh(B\zeta)$$

for case 2) is shown at $T = 0$.

The numerical channel is $X = 8$ dimensionless units long if $Y = 1$ is its width. For the chosen mode, the Rossby number and aspect ratio are

$$\epsilon = \delta_1^2 = L_y^2/L_x^2 = (B/2)^2 = 0.25.$$

In Fig. 7 the initial evolution of the given initial con-

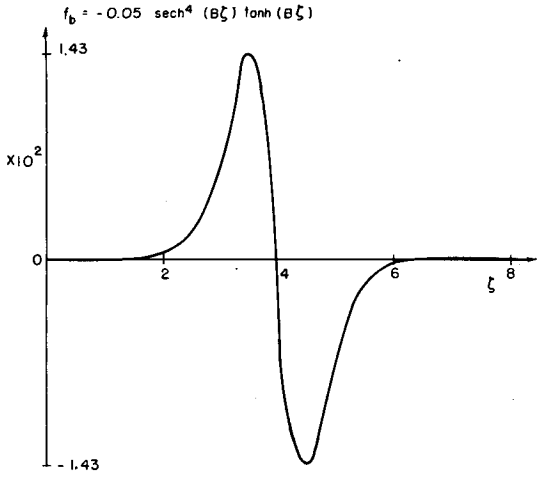

FIG. 6. Shape of the forcing function $f_b = -0.05\ \mathrm{sech}^4(B\zeta)$ $\tanh(B\zeta)$ in the channel $1 \leq \zeta \leq 8$ with $B = 1$.

dition is shown in the reference frame of (3.24), moving with the northern forcing wave. The slow distortion of the initial wave under the asymmetric forcing function is evident. After $n = 320$ time steps, the forced response has become completely asymmetric. Its amplitude continues to grow because the model has no dissipation. After $n \sim 960$ time steps, the forced response begins to break down into a number of high amplitude nonlinear pulses. With a time step $DT = 10^{-3}$ required for numerical stability, this corresponds to a long time scale $T \approx \mathrm{O}(1)$ or $t \approx 4$ on the short time scale. In Figs. 8a and b we show the evolution of the given initial condition after breakdown. Specifically, Fig. 8a shows the initial condition itself and its shape after $n = 320$ time steps, when it has become asymmetric. The two successive responses are at $n = 1280$ and $n = 2240$ time steps. It can be noticed that the response breaks down first on the side where its amplitude has become positive under the influence of the forcing. However, the nonlinear pulses thus produced decay rapidly when emerging from the region in the channel directly affected by the forcing. Figure 8b shows the successive evolution at $n = 2880$ and $n = 3520$ time steps, at which the numerical experiments were ended. The behavior of the forced response now shows some remarkable features. On the side where the forced response has become positive, namely the left part of the channel, the pulses which are produced rapidly decay to very small amplitude as soon as they emerge from the region directly affected by the forcing. Each nonlinear pulse also moves westward while rapidly decreasing, as is evident when comparing the evolution at $n = 2880$ with that at $n = 3520$. At the center of the channel the forced response is biggest, and its maximum amplitude shifts eastward in the final stages of the experiment. On the right part of the channel, where the forced wave was still negative at $T \sim \mathrm{O}(1)$, the behavior is very different. Nonlinear pulses also are produced but 1) they move eastward, and 2) they are much more regular in space and they increase in amplitude from time step $n = 2880$ to $n = 3520$. Notice that the regularly spaced pulses have high amplitudes exactly out of the region of direct forcing influence.

The above result is consistent with the properties of the time-dependent unforced KdV equation. As previously noted, the free nonlinear steady solitary wave would have $A \sim -0.4$ in the present experiment. Also, its (constant) nonlinear phase speed would be $c_1 \sim \frac{1}{3}$, namely an eastward correction to the linear phase speed $c_0 \approx -\frac{1}{6}$. When the forced response pulses emerge from the direct forcing influence, they will behave like free nonlinear waves. In the channel region, where at $T \sim \mathrm{O}(1)$ the forced amplitude is still negative, they will be allowed to evolve as free solitons of the KdV equation. In the opposite region, instead, they will rapidly decay to dispersive wave packets. Also, the free nonlinear pulses in the right region of the channel move eastward. Note that the forced response is represented in the reference frame moving with the linear phase speed $c_0 \approx -\frac{1}{6}$. The limited length of the channel and the periodic boundary conditions prevent a better separation of the free nonlinear waves on the one side from the dispersive decaying radiation on the other.

Let us now interpret the above results as resonant radiation propagating away from the northern moving boundary in the zonal channel. The boundary wave is moving westward; thus a radiating forced response is allowed in the present weakly nonlinear case. The boundary wave also undergoes a slow modulation over a long time scale T. The forced response will then exhibit a nonlinear cascade of energy to wavelengths smaller than the initial wavelength $L_x = 1/B$ determined by the forcing wave. This cascade is deterministic. As the forcing has a limited spatial extent, the

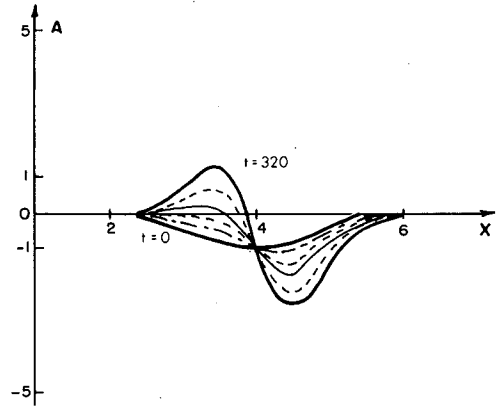

FIG. 7. Evolution of the initial condition $g(\zeta) = A\ \mathrm{sech}^2(B\zeta)$, with $B = 1$ and $A = -1$ in the reference frame moving with the forcing wave at the initial state $t = 0$, and at the successive dimensionless times $t = 60$, 180 and 240, and at the completely asymmetric state $t = 320$.

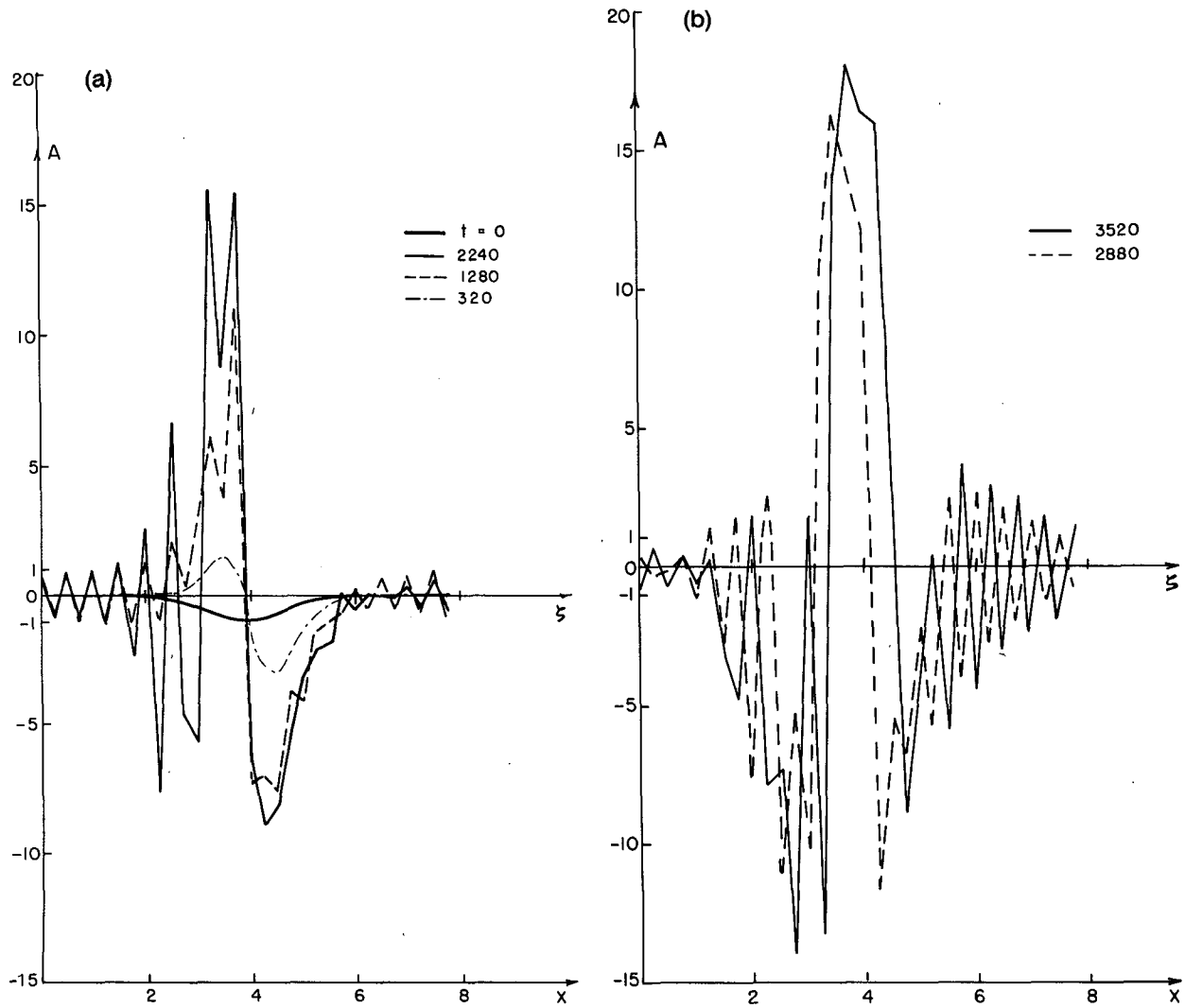

FIG. 8. Evolution of the initial condition of Fig. 7 on the long time scale T. (a) Initial condition at $t = 0$ and successive evolution at the labeled dimensionless times. (b) Successive evolution of the pattern of (a) at the labeled dimensionless times.

forced nonlinear eddies will evolve according to the different types of dynamics as soon as they are outside the region directly affected by the forcing. In the region in which the forced amplitude has the same sign as the allowed free nonlinear waves, the smaller eddies produced will evolve as free permanent-form nonlinear structures. In the present case they are slower than the boundary wave. Conversely, in the opposite region they will obey a dispersive dynamics. In the present case, the dispersive wave packets are faster than the boundary wave. The final pattern will be composed of a forced wave resonantly excited, radiating from the moving northern boundary and breaking into smaller and slower nonlinear eddies, together with dispersive faster radiation. The above picture seems to be a consistent, though qualitative, model for regions of intense mesoscale activity south of a moving boundary current.

4. Conclusions

In this study we analyze the effects of nonlinearity in determining the properties of free and boundary-forced radiation in a zonal channel in the context of a simple analytical model. The results of this investigation can be summarized as follows:

1) Nonlinear, permanent-form free solutions are allowed for by the model in a variety of parameter ranges. In the weak nonlinear limit these solutions are nonlinear topographic Rossby waves asymmetric in the zonal direction. In the limit of high nonlinearity, the steady free solution is a radially symmetric monopole with closed recirculation regions. The shape is that typical of coherent eddies which have been observed to be shed by an unstable eastward-flowing jet like the Gulf Stream.

2) For the boundary-forced case, a meandering current is idealized as a moving northern boundary. The weakly nonlinear case has been thoroughly investigated over an arbitrary relief $h(y)$. The most important effect of nonlinearity is to allow for the production of nonlinear radiation in the interior field through a resonance mechanism. In the corresponding linear model the interior response would be infinite. The resonant, equilibrium-forced solutions obey a forced KdV equation, which can be solved in general only numerically. Analytical solutions can be found for a specific shape of the northern forcing wave. Under this assumption, it can be shown that the resonant interior response has multiple equilibria, that is, two equilibrium amplitudes for quite general values of the nonlinear phase speed $c_1(A)$.

3) Always in the weakly nonlinear limit, a second important effect of nonlinearity can be investigated allowing for a slow time modulation of the northern wall forcing. The resonant interior response then obeys a time-dependent KdV equation. An initial condition corresponding to the steady equilibrium solution valid in the same parameter range evolves with soliton production under the influence of the modulated forcing. When the produced solitons emerge from the region directly affected by the forcing, they propagate as free permanent radiation in the direction allowed for by the unforced KdV model. In the opposite direction they evolve into dispersive wave packets. Thus, the resonant interior response undergoes, on the long time scale, a nonlinear, deterministic cascade process leading to nonlinear radiation of shorter wavelength, smaller eddies, together with dispersive radiation. These two types of radiation travel with opposite phase speeds with respect to the boundary wave.

4) The highly nonlinear, boundary-forced case can be studied analytically only in the limit of high nonlinearity (Ro = 1) but small north–south to east–west aspect ratio ($\delta_1^2 \ll 1$). This corresponds to the case of resonantly excited long-wavelength radiation in the zonal channel. Nonlinearity can be shown to modify profoundly the interior field with respect to the purely linear model. In the linear case, over a relief which is essentially northward sloping, an eastward-moving boundary wave excites a response which, at best, has an oscillatory nature only in some interior, limited region. Near the northern boundary itself, this response decays exponentially to zero. Conversely, in the highly nonlinear case the resonant response is shown to have an oscillatory behavior near the northern boundary even when this boundary is eastward moving. Thus, the limit of high nonlinearity also will allow radiation to propagate into the far field from an eastward-moving meandering current. In the limit $\delta_1^2 \to 1$, the excited nonlinear eddy would tend to the monopole shape of Fig. 1 with closed recirculation regions and might detach from the boundary, propagating like a Gulf Stream ring.

The fully nonlinear case, with an aspect ratio $\delta_1^2 = O(1)$, cannot be treated in the context of the present asymptotic theory. It can be explored only through numerical experiments carried out by directly integrating the full model in the different parameter ranges of physical significance. Numerical experiments are therefore necessary to explore the possibility that a nonlinear resonant mechanism like the one proposed here will excite interior radiation profoundly different from that produced in the context of a linear theory. Such experiments should 1) allow for radiating solutions when the northern jet is eastward moving, and 2) allow for eddy shapes to be excited, similar to the free monopole solutions found in Section 1. Progress in this direction is already under way.

Acknowledgment. This research was carried out with the support of the National Science Foundation under Grant OCE-8118473.

APPENDIX

Solution of (3.16) Near the Northern Boundary

The starting equation is

$$\psi_{0yys} - \frac{1 + c_0 + h_y}{c_0}\psi_{0s} - \frac{1}{c_0}(\psi_{0s}\psi_{0yyy} - \psi_{0y}\psi_{0yys}) = 0. \tag{A1}$$

We want to explore the behavior of (A1) near the northern boundary where $y = 1$. The change of coordinate is

$$y' = y - 1.$$

Equation (A1) remains formally identical in the new coordinate y':

$$\psi_{0y'y's} - \frac{1 + c_0 + h'_y}{c_0}\psi_{0s} - \frac{1}{c_0}(\psi_{0s}\psi_{0y'y'y'} - \psi_{0y'}\psi_{0y'y's}) = 0. \tag{A1a}$$

Put

$$\psi_{0y'y'} = F(\psi_0, y'), \tag{A2}$$

an unknown functional of the two arguments (ψ_0, y). Then

$$1)\ \psi_{0y'y's} = J(\psi_{0y'y'}, y') = \frac{\partial F}{\partial \psi_0}\psi_{0s}$$

$$= J\left(\psi_0, \frac{\partial F}{\partial \psi_0}y'\right) - J\left(\psi_0, \frac{\partial^2 F}{\partial \psi_0 \partial y'}\frac{y'^2}{2}\right)$$

$$+ J\left(\psi_0, \frac{\partial^3 F}{\partial \psi_0 \partial y'^2}\frac{y'^3}{6}\right) - J\left(\psi_0, \frac{\partial^4 F}{\partial \psi_0 \partial y'^3}\frac{y'^4}{24}\right) + \cdots,$$

$$2)\ J(\psi_0, \psi_{0y'y'}) = J[\psi_0, F(\psi_0, y')] \neq 0,$$

and (A1a) becomes

$$J\left(\psi_0, \left\{\frac{\partial F}{\partial \psi_0} y' - \frac{\partial^2 F}{\partial \psi_0 \partial y'} \frac{y'^2}{2} + \frac{\partial^3 F}{\partial \psi_0 \partial y'^2} \frac{y'^3}{6} - \frac{\partial^4 F}{\partial \psi_0 \partial y'^3} \frac{y'^4}{24} + \cdots - \frac{(1+c_0)y' + h(y')}{c_0} - \frac{1}{c_0} F(\psi_0, y')\right\}\right) = 0,$$

or

$$\frac{\partial F}{\partial \psi_0} y' - \frac{\partial^2 F}{\partial \psi_0 \partial y'} \frac{y'^2}{2} + \frac{\partial^3 F}{\partial \psi_0 \partial y'^2} \frac{y'^3}{6} - \frac{\partial^4 F}{\partial \psi_0 \partial y'^3} \frac{y'^4}{24} + \cdots - \frac{(1+c_0)y' + h(y')}{c_0} - \frac{1}{c_0} F(\psi_0, y') = G(\psi_0). \quad \text{(A3)}$$

The general solution of (A3) is

$$F = F_H + F_p,$$

where F_H is the integral of the homogeneous part of (A3) and F_p is a particular integral depending on the unknown function $G(\psi_0)$.

We seek a particular integral of (A3) in the form

$$F_p = aX(\psi_0) + b(y')$$

for which

$$\frac{\partial^2 F}{\partial \psi_0 \partial y'} = \frac{\partial^3 F}{\partial \psi_0 \partial y'^2} = \cdots = 0.$$

Equation (A3) is then exactly

$$\frac{\partial F_p}{\partial \psi_0} y' - \frac{(1+c_0)y' + h(y')}{c_0} - \frac{1}{c_0} F_p = G(\psi_0). \quad \text{(A4)}$$

Substituting the expression for F_p into (A4),

$$ay' \frac{dX}{d\psi_0} - \frac{(1+c_0)y' + h(y')}{c_0} - \frac{a}{c_0} X(\psi_0) - \frac{b(y')}{c_0} = G(\psi_0). \quad \text{(A5a)}$$

Differentiating once with respect to ψ_0,

$$ay' \frac{d^2X}{d\psi_0^2} = \frac{d}{d\psi_0}\left[\frac{a}{c_0} X + G\right].$$

The above identity admits no solution unless

$$\frac{d^2X}{d\psi_0^2} = 0, \quad \frac{d}{d\psi_0}\left[\frac{a}{c_0} X + G\right] = 0. \quad \text{(A5b)}$$

The solutions of (A5b) are

$$\left.\begin{aligned} X &= p\psi_0 + q \\ G &= r - \frac{a}{c_0}(p\psi_0 + q) \end{aligned}\right\}, \quad \text{(A5c)}$$

where p, q and r are integration constants. Substituting (A5c) into (A5a) we get

$$\frac{b(y')}{c_0} = apy' - \frac{(1+c_0)y' + h(y')}{c_0} - r.$$

With no loss of generality, take

$$r \equiv 0, \quad a \equiv 1, \quad p \equiv 1, \quad q \equiv 0,$$

so

$$b(y') = c_0 y' - [(1+c_0)y' + h(y')] = -[y' + h(y')]$$

and

$$F_p = \psi_0 - [y' + h(y')]. \quad \text{(A6)}$$

To evaluate the homogeneous integral F_H the following approximation is made. We want to explore the behavior of the solution to (A1a) near the northern boundary $y' = 0$, in a region where: $\cdots y'^4 \ll y'^3 \ll y'^2 \ll y'$. In this region we can approximate (A3), retaining only the terms $O(y')$. Near the northern boundary $y' = 0$ the equation for F_H is then

$$\frac{\partial F_H}{\partial \psi_0} y' - \frac{(1+c_0)y' + h(y')}{c_0} - \frac{1}{c_0} F_H(\psi_0, y') \approx 0. \quad \text{(A7)}$$

Differentiating with respect to ψ_0,

$$y' \frac{\partial^2 F_H}{\partial \psi_0^2} - \frac{1}{c_0} \frac{\partial F_H}{\partial \psi_0} \approx 0,$$

the solution of which is

$$\frac{\partial F_H}{\partial \psi_0} \approx H(y') \exp(\psi_0/c_0 y'). \quad \text{(A8a)}$$

But from (A7),

$$\frac{\partial F_H}{\partial \psi_0} \approx \frac{(1+c_0)y' + h(y')}{c_0} + \frac{F_H}{c_0 y'}. \quad \text{(A8b)}$$

Equations (A8a) and (A8b) give

$$F_H(\psi_0, y') \approx c_0 y' H(y') \exp(\psi_0/c_0 y') - [(1+c_0)y' + h(y')] \quad \text{(A8c)}$$

near the northern boundary.

We now require ψ_0 to be a localized structure in s, namely

$$\psi_0 \to 0 \quad \text{as} \quad s \to \pm\infty.$$

From

$$\frac{\partial F_{H\infty}}{\partial \psi_0} = \lim_{s\to\infty} \frac{\partial F_H}{\partial \psi_0} = \lim_{\psi_0 \to 0} H(y') \exp(\psi_0/c_0 y') = H(y'),$$

it follows that

$$F_{H\infty} = H(y')\psi_{0\infty} + K(y) \to K(y) \quad \text{as} \quad \psi_{0\infty} \to 0.$$

Without loss of generality, take the arbitrary constant $K(y) \equiv 0$. Then

$$F_{H\infty} = \lim_{s\to\infty} F_H \to 0.$$

From (A8c) in the limit $s \to \pm\infty$, we obtain

$$H(y') = \frac{(1 + c_0)y' + h(y')}{c_0 y'}.$$

Because $F_H(\psi_0, y')$ is an analytical functional, we finally have

$$F_H(\psi_0, y') \approx [(1 + c_0)y' + h(y')][\exp(\psi_0/c_0 y') - 1]. \tag{A9}$$

The complete, approximate solution valid near the northern boundary is then

$$\psi_{0y'y'} = F(\psi_0, y') = F_H + F_p \approx [(1 + c_0)y' + h(y')][\exp(\psi_0/c_0 y') - 1] + \psi_0 - [y' + h(y')].$$

REFERENCES

Flierl, G. R., 1979a: Planetary solitary waves. *POLYMODE News,* No. 62, WHOI, 1–5.

——, 1979b: Baroclinic solitary waves with radial symmetry. *Dyn. Atmos. Oceans,* **3,** 15–38.

——, V. M. Kamenkovich and A. R. Robinson, 1975: Gulf Stream meandering and Gulf Stream rings. Dynamics and the analysis of MODE-1. Unpublished manuscript, MODE Dynamics Group, MIT, 113–135.

——, V. D. Larichev, J. C. McWilliams and G. M. Reznik, 1980: The dynamics of baroclinic and barotropic solitary eddies. *Dyn. Atmos. Oceans,* **5,** 1–41.

Fornberg, G., and G. B. Whitham, 1978: A numerical and theoretical study of certain nonlinear wave phenomena. *Proc. Roy. Soc. London,* **A289,** 373–403.

Harrison, D. E., and A. R. Robinson, 1979: Boundary-forced planetary waves: A simple model of mid-ocean response to strong current variability. *J. Phys. Oceanogr.,* **9,** 919–929.

Holland, W. R., 1978: The role of mesoscale eddies in the general circulation of the ocean: Numerical experiments using a quasi-geostrophic model. *J. Phys. Oceanogr.,* **8,** 363–392.

Ikeda, M., 1981: Meanders and detached eddies of a strong eastward-flowing jet using a two-layer quasi-geostrophic model. *J. Phys. Oceanogr.,* **11,** 526–540.

——, and J. R. Apel, 1981: Mesoscale eddies detached from spatially growing meanders in an eastward-flowing oceanic jet using a two-layer quasi-geostrophic model. *J. Phys. Oceanogr.,* **11,** 1638–1661.

Jeffrey, A., and T. Kakutani, 1972: Weak nonlinear dispersive waves: A discussion centered around the Korteweg–deVries equation. *SIAM Rev.,* **14,** 582–643.

Larichev, V. D., and G. M. Reznik, 1976: Two-dimensional Rossby soliton: An exact solution. *POLYMODE News,* No. 19, WHOI, 1–3.

Malanotte-Rizzoli, P., 1980a: Planetary solitary waves over variable relief: A unified approach. *POLYMODE News,* No. 75, WHOI, 1–6.

——, 1980b: Solitary Rossby waves over variable relief and their stability. Part II: Numerical experiments. *Dyn. Atmos. Oceans,* **4,** 261–294.

——, 1982: Planetary solitary waves in geophysical flows. *Advances in Geophysics,* Vol. 24, Academic Press, 147–224.

Miles, J. W., 1979: On the Korteweg–deVries equation for a gradually varying channel. *J. Fluid Mech.,* **91,** 181–190.

Pedlosky, J., 1977: On the radiation of mesoscale energy in the mid-ocean. *Deep-Sea Res.,* **24,** 591–600.

Zabusky, N. J., and M. D. Kruskal, 1965: Interaction of solitons in a collisionless plasma and the recurrence of initial states. *Phys. Rev. Lett.,* **15,** 240–243.